CITC GLOBAL
Construction in the 21st Century

The Fifteenth International Conference on Construction in the 21st Century (CITC-15)
Rabat, Morocco | November 10 - 14, 2025

Solar-Powered Site Operations for Net-Zero Construction Projects

Odey Alshboul[1], Ali Shehadeh [2], Ghassan Almasabha[3]

[1]Department of Civil Engineering, Faculty of Engineering, The Hashemite University, P.O. Box 330127, Zarqa 13133, Jordan (corresponding author) odey.shboul@hu.edu.jo
[2] Department of Civil Engineering, Hijjawi Faculty for Engineering Technology, Yarmouk University, P.O. Box 566, Irbid 21163, Jordan. ali.shehadeh@yu.edu.jo
[3] Department of Civil Engineering, Faculty of Engineering, The Hashemite University, P.O. Box 330127, Zarqa 13133, Jordan. ghassans@hu.edu.jo

Abstract
This paper targets the construction phase itself as a lever for achieving NZEC at Yarmouk University. We propose and test a site-microgrid strategy that couples campus PV generation, portable battery systems, and electrified equipment to displace diesel use during capital works. Time-synchronized campus export data inform a forecasting layer (LSTM) that predicts PV availability and background demand; these forecasts feed a mixed-integer optimization that co-schedule high-energy construction tasks (lifting, mixing, cutting, temporary HVAC) with battery dispatch and grid import limits. The framework includes power-quality and safety constraints for cranes and heavy tools, and contract clauses (SLAs, green KPIs) that align contractors' operations with campus energy windows. Scenario analysis demonstrates that aligning task timing and microgrid dispatch can materially reduce fuel consumption, noise, and emissions while maintaining productivity and compliance. The result is a replicable blueprint for solarized construction operations that accelerates NZEC targets and embeds decarbonization into project delivery, not only building performance.

Keywords
construction site energy; schedule optimization; low-carbon procurement; Net Zero Energy Campus

1. Introduction

Universities pursuing Net Zero Energy Campus (NZEC) targets have largely concentrated on permanent buildings and utility system retrofits, high-performance envelopes, and large-scale photovoltaics with storage (Maghami et al., 2025). Far less attention has been paid to the construction phase itself, even though capital works introduce temporary loads, diesel generators, and idling equipment that can materially erode campus-wide carbon gains. On most projects, lifting, mixing, cutting, dewatering, and temporary HVAC are scheduled for productivity and access alone, with energy treated as an externality (Kanafani et al., 2023). While there has been more and more interest in the Net Zero Energy Building (NZEB) concept over recent years, many reports recommend that much more study and examination is necessary (Cielo & Subiantoro, 2021; Li et al., 2013). Therefore, it is necessary to continue genuine scholarly inquiry, and based on such findings, the actual practice and growth of NZEB to its full capacity in supporting sustainable development (Jaysawal et al., 2022; Maduta et al., 2025; Parvin et al., 2025). This is an important gap in campus contexts, where projects are frequent, proximate to occupied building facilities, and subject to interactions with on-site renewable generation that are often curtailed or exported at low value during midday peak output. Utilizing those solar opportunities to offset construction operations presents a direct near-term strategy to eliminate fuel, reduce noise and local air quality emissions, while managing consideration for schedule and safety (Nwagu et al., 2025).

This paper targets that overlooked lever. We develop and test a site-microgrid strategy for Yarmouk University that couples existing campus PV generation with portable battery systems and electrified equipment to displace diesel during construction. The core challenge is temporal: PV availability and background campus demand

fluctuate at sub-hourly scales; construction tasks have precedence, crew, and resource constraints; and power-quality requirements for cranes and heavy tools impose limits on inrush current, voltage sag, and harmonics. Treating these interactions piecemeal leads either to lost decarbonization potential (over-conservatism) or unsafe/uneconomic operations (over-optimism). What is needed is an integrated framework that forecasts supply and demand, then co-optimizes task timing and microgrid dispatch subject to safety and quality constraints and finally embeds those operational rules into contract mechanisms that align contractor behavior with campus energy windows.

We recommend a two-layer architecture. A forecasting layer utilizes time-coincident campus export data to provide training for a sequence model (LSTM) that predicts short-horizon PV availability and net load. The predictions made from this model provide input to a mixed-integer optimization model that schedules energy-expensive tasks (e.g., crane lifts, concrete mixing, metal cutting, temporary HVAC) in conjunction with battery charge/discharge constraints, and grid import caps. The mixed-integer optimization model accounts for crew calendars and task precedence, noise curfews, demand-shaping objectives, and maintains headroom for ultra-reliable power quality constraints and emergency operations. To close the loop between the plan and actual practice, we translate the solutions into the language of contracts—service level agreements (SLAs) and green key performance indicators (KPIs)—that prescribe allowable import bands, emissions limits, and compliance reporting, with incentive arrangements for compliance and penalties for noncompliance.

Our contributions are threefold. First, we frame "solarized construction operations" as a replicable microgrid-scheduling problem that explicitly couples construction planning with campus energy management. Second, we operationalize this framing with a data-driven pipeline—LSTM forecasting plus mixed-integer co-scheduling—that respects the realities of site logistics, power quality, and safety. Third, we demonstrate, through scenario analysis on real campus data, that aligning task timing with PV-battery dispatch can materially reduce diesel consumption and acoustic impacts without compromising productivity or regulatory compliance. While the case study is situated at Yarmouk University, the method generalizes to any campus or portfolio owner integrating renewables and seeking to embed decarbonization into project delivery, not just building performance. By treating construction as an energy-aware process, NZEC becomes not only an outcome of what is built, but also of how it is built.

2. Methods

This study develops and tests a two-layer, data-driven framework that solarizes construction operations by aligning site activities with campus PV availability. Layer 1 forecasts short-horizon PV output and campus net load using time-synchronized meter data. Layer 2 solves a mixed-integer optimization that co-schedules high-energy construction tasks with battery dispatch and grid-import limits while enforcing power-quality and safety constraints. We parameterize task energy profiles and operational constraints using a multi-site dataset of U.S. construction projects and apply the model to Yarmouk University (YU) campus operations for scenario evaluation.

We adopted an applied quantitative design combining: (i) supervised time-series forecasting (sequence learning) for supply/demand prediction; (ii) mixed-integer linear programming (MILP) for joint activity-energy scheduling; and (iii) quasi-experimental scenario analysis comparing baseline diesel-driven operations with solar-microgrid strategies. The approach is explanatory (to identify drivers of diesel displacement and import-band compliance) and prescriptive (to compute optimal schedules/dispatch under constraints). A compact mathematical model (below) formalizes co-scheduling, and a rolling-horizon controller implements forecasts-in-the-loop.

We combine three complementary data blocks. First, the campus energy telemetry for the Yarmouk University (YU) case environment consists of one-minute PV export and net-load time series from the campus supervisory system, augmented by local weather (global horizontal irradiance, ambient temperature, cloud cover), calendar markers (weekday/weekend, teaching vs. exam periods), and grid-side constraints (import caps, planned outage windows). Second, a U.S. construction activity & equipment telemetry reference set (2018–2024) provides minute-level temporary-power submetering, crane/welder/compactor telematics, e-ticket timestamps for concrete/asphalt, crew rosters, and noise-curfew logs across capital works executed on or adjacent to university, healthcare, and municipal campuses spanning seven ASHRAE climate zones. Third, asset specifications supply portable BESS ratings (kW/kWh, round-trip efficiency, charge/discharge limits), protection settings (breaker curves, RCD/GFCI), and recommended inrush/THD limits relevant to heavy tools and variable-frequency drives.

All-time series are aligned to a 1-minute grid and stored using the Asia/Amman offset (UTC+03:00) for YU. We exclude intervals with >20% substream missingness; remaining gaps up to 10 consecutive minutes are imputed with Kalman smoothing, while longer gaps are masked and withheld from model training but retained as uncertainty bands for optimization and sensitivity analysis. Task logs are normalized to atomic activities with attributes—earliest start, nominal duration, crew type/size, base power, surge multiplier, location (to estimate cable run/proximity), and curfew flags. Power traces are aggregated as piecewise-constant demand profiles with explicit inrush windows tagged to respect protection and THD limits during scheduling.

The U.S. reference set is constructed via stratified random sampling by (i) ASHRAE climate zone (7 strata), (ii) project archetype (academic building, laboratory, utility/infrastructure, landscape/hardscape), and (iii) season of peak activity. Within each stratum, eligible projects were those with ≥4 weeks of synchronized temp-power metering or tool telematics, documented noise-curfew rules, and recorded crane or mixing operations. Of 132 candidates, 96 passed data-quality screens (72.7% retention), forming the analytical sample. The YU case adopts a purposive sample of construction work packages scheduled during high-PV months to stress-test the scheduling and site-microgrid strategy under realistic campus constraints.

Table 1 summarizes holistic descriptive statistics and site constraints used to calibrate and validate the scheduling and microgrid optimization engine. Variables are defined alongside their sources; where distributional moments are meaningful, we report means, standard deviations, and 10th/90th percentiles to bound realistic operating envelopes for loads, surges, feeder limits, and storage.

Table 1. Descriptive statistics

Item	Definition	Source	N / Value	Mean	SD	P10	P90
Projects (U.S.)	Eligible work with temp-power metering	Multi-site dataset	96	—	—	—	—
Climate zones	ASHRAE zones represented	Categorical	7	—	—	—	—
Atomic task records	Distinct lifts/mixes/cuts/HVAC segments	U.S. dataset	58,240	—	—	—	—
Task duration (min)	Start-to-end per atomic task	U.S. dataset	—	42	28	12	95
Peak task power (kW)	Nameplate × utilization	U.S. dataset	—	52	31	12	110
Inrush multiplier (×)	Short-term surge vs. running	U.S. dataset	—	2.9	0.6	2.1	3.8
Temp HVAC hours/day	Operating hours during works	U.S. dataset	—	6.0	3.0	2.0	10.0
Crane lifts/day	Count of lifting tasks	U.S. dataset	—	8	5	2	18
Mixing tasks/day	Concrete/asphalt batching cycles	U.S. dataset	—	6	4	1	13
Cutting/welding tasks/day	Metal/stone tool use	U.S. dataset	—	12	7	3	24
Baseline diesel (L/day)	Generator/plant fuel use	U.S. dataset	—	185	90	70	340
Import cap (kW)	Temp feeder capacity limit	Site records	—	120	40	60	180
BESS energy (kWh)	Portable battery capacity	Asset specs	—	250	120	96	480
BESS power (kW)	Continuous charge/discharge	Asset specs	—	100	45	40	180
PV window overlap (%)	Share of 07:00–17:00 with PV>threshold	Weather+PV proxy	—	46	12	28	63
Data missingness (%)	Fraction of minutes with gaps	All streams	—	3.0	2.0	0.8	6.5

The proposed model formalizes solar-powered site operations as a coupled forecasting–optimization system that aligns construction task timing with campus PV and portable storage. A probabilistic LSTM produces calibrated PV and net-load trajectories, which are transformed into correlated scenarios. These feed a mixed-integer program that enforces construction logic (durations, precedence, crews, curfews) while co-optimizing grid import, PV inverter setpoints, and BESS charge/discharge. Power-quality and safety are embedded via linearized voltage-sag, harmonic, and feeder-ampacity guardrails; risk is controlled through CVaR constraints on import-band breaches. A multi-objective function trades cost, emissions, power-quality incidents, and schedule stability to yield implementable minute-level plans.

Eq. (1) is vital to anticipate minute-ahead PV availability and campus net load that drive co-scheduling. We use a sequence model with gates and quantile heads so the optimizer can reason about uncertainty rather than just point estimates. Let z_t stack recent meter lags, weather nowcasts, and calendar/site indicators; $\hat{y}_{t+h|t}(\tau)$ returns τ-quantiles for (p_{pv}, ℓ_{campus}) at horizon $h \in \{5,15,30,60\}$ minutes.

$$i_t = \sigma(W_i z_t + U_i h_{t-1} + b_i), f_t = \sigma\left(W_f z_t + U_f h_{t-1} + b_f\right) \quad (1)$$

Here σ is the logistic function, $W_\cdot, U_\cdot, b_\cdot$ are learned parameters, and h_t is the hidden state.

To preserve cross-dependence between PV and campus load (e.g., cloud passage during exams), we transform Eq. (1) quantiles into correlated scenarios as shown in Eq. (2).

$$s_{t+h}^{(k)} = \mu_{t+h} + F^{-1}\left(\Phi\left(L\, u^{(k)}\right)\right) \quad (2)$$

where μ_{t+h} stacks median forecasts, F^{-1} is the vector of inverse marginals for Φ is the standard normal.

We encode construction logic by convolving start decisions with task durations and enforcing precedence. For tasks i with integer duration d_i minutes and feasible window as shown in Eq. (3).

$$y_{i,t} = \sum_{\tau=0}^{d_i-1} x_{i,t-\tau}, \qquad \sum_t x_{i,t} = 1, \qquad \sum_t (t+d_i)x_{i,t} \le \sum_t t\, x_{j,t} \quad \forall (i \prec j) \tag{3}$$

where $x_{i,t} \in \{0,1\}$ indicates "task i starts at t", and $y_{i,t} \in \{0,1\}$ indicates "task i active at t". This equation is critical to keep crew-level feasibility while allowing the energy system to reshape when, not whether, high-energy tasks occur.

High-power site tools exhibit short inrush periods that must be planned explicitly to avoid sags. Let $\chi_{i,t} \le y_{i,t}$ indicate whether task i is in its surge sub-window, with surge factor $\kappa_i \ge 1$ as shown in Eq. (4).

$$p_t^{grid} + p_t^{dis} + p_t^{inv} = \sum_i p_i\, y_{i,t} + \sum_i (\kappa_i - 1) p_i\, \chi_{i,t} + p_t^{ch} + r_t \tag{4}$$

where p_t^{grid} is grid import, p_t^{dis}/p_t^{ch} are BESS discharge/charge, $p_t^{inv} \le \min\{\hat{p}_{pv}^{\,t},\ \bar{p}_{inv}\}$ is inverter-limited PV injection, p_i is task running power, and r_t is spinning reserve. This equation is critical to enforce instantaneous feasibility, explicitly separating steady running power from surge contributions.

Beyond energy balance, we penalize cycling-induced degradation as shown in Eq. (5). With sampling period Δt, charge/discharge efficiencies η_{ch}, η_{dis}.

$$E_{t+1} = E_t + \eta_{ch}\, p_t^{ch}\, \Delta t - \frac{1}{\eta_{dis}}\, p_t^{dis}\, \Delta t \tag{5}$$

where $\alpha, \beta \ge 0$ tune cycle-throughput and SOC-deviation penalties, and $\bar{E}$ is a health-preserving mid-SOC.

We protect cranes and large drives by bounding voltage depression during surges through feeder impedances R, X relative to nominal V_0. Let total active/reactive injections be P_t, Q_t as shown in Eq. (6),

$$\Delta V_t \approx \frac{R}{V_0}\, P_t + \frac{X}{V_0}\, Q_t \le \overline{\Delta V}, \qquad P_t = \sum_i \kappa_i p_i \chi_{i,t} + \sum_i p_i y_{i,t} - p_t^{inv} - p_t^{dis} + p_t^{ch} \tag{6}$$

with $\overline{\Delta V}$ the allowable sag (e.g., 8–10%).

Some tools inject harmonics; we cap total harmonic distortion (THD) using device-level spectral factors $\phi_{i,h}$ per harmonic $h \ge 2$ as shown in Eq. (7).

$$THD_t = \sum_{h=2}^{H} \left(\frac{I_{h,t}}{I_{1,t}}\right)^2 \le \overline{THD}, \qquad I_{h,t} = \sum_i \phi_{i,h}\, y_{i,t}, \qquad I_{1,t} \propto \frac{P_t}{V_0} \tag{7}$$

where $I_{1,t}$ is the fundamental current magnitude. This equation is critical to keep flicker and overheating within practice standards when concentrating cutting/welding windows around PV peaks.

We control the tail risk of breaching grid import bands under forecast error using a convex CVaR construction in Eq. (8). For scenario $k = 1, \dots, K$ with import overage $g_t^{(k)} = \max\{0,\ p_t^{grid\,(k)} - \bar{p}_t^{grid}\}$.

$$\min_{z_t, u_t^{(k)} \ge 0} \quad z_t + \frac{1}{(1-\alpha)K} \sum_{k=1}^{K} u_t^{(k)} \qquad \text{s.t.} \quad u_t^{(k)} \ge g_t^{(k)} - z_t, \quad \forall k, \qquad \forall t, \tag{8}$$

with confidence level $\alpha \in (0,1)$.

To respect the PV inverter's apparent-power limit $\bar{S}_{inv}$ while providing reactive, we impose the standard capability circle in SOC form as shown in Eq. (9).

$$\left\| \begin{bmatrix} Q_t^{inv} \\ P_t^{inv} - \frac{\bar{S}_{inv}}{2} \end{bmatrix} \right\|_2 \leq \frac{\bar{S}_{inv}}{2}, \qquad 0 \leq P_t^{inv} \leq \min\{\hat{p}_{pv}^t, \quad \bar{p}_{inv}\} \tag{9}$$

where $P_t^{inv} = p_t^{inv}$ and Q_t^{inv} is commanded reactive power. This equation is critical to co-optimize active PV injection with voltage support, expanding feasible windows for heavy lifts without diesel.

Finally we scalarize cost, carbon, power-quality penalties, and lateness, while discouraging excessive rescheduling between rolling horizons via a trust-region on starts. Let $x_{i,t}^{ref}$ be the previous horizon's plan; $\rho > 0$ controls "chatter" as shown in Eq. (10).

$$\min \underbrace{\sum_t w_{cost}\, c_t\, p_t^{grid}}_{\text{energy}} + \underbrace{\sum_t w_{co2}\, (e_{grid}\, p_t^{grid} + e_{diesel}\, p_t^{diesel} + \gamma\, C_{deg})}_{\text{emissions+aging}}$$
$$+ \underbrace{\textstyle\sum_t w_{pq} \left(\frac{\Delta V_t}{\overline{\Delta V}} + \frac{THD_t}{\overline{THD}} \right)}_{\text{powerquality}} + \underbrace{\textstyle\sum_i w_{late}\, L_i}_{\text{schedule}} + \underbrace{\rho \textstyle\sum_{i,t} |x_{i,t} - x_{i,t}^{ref}|}_{\text{stability}} \tag{10}$$

where c_t is tariff or implicit cost, $e_{\cdot}$ are emission factors, γ scales BESS aging into CO_2e-equivalent, and L_i penalizes tardy starts. This equation is critical to internalize low-carbon procurement goals (cost+CO_2e), safety/quality (voltage/harmonics), and practical site management (stable crew plans).

The equations guarantee that the electrical performance is instantaneous, that meeting campus import boundaries is assured, and that construction and operation can be considered under uncertainty—inclusive of every alternative represented. The optimizer generates (i) starts and windows of activity that are crew-ready tasks, (ii) inverter and battery dispatch setpoints with necessary reserves for SOC, and (iii) KPI forecasts of diesel displaced, CO_2e reduction, import-band adherence, and avoidance of noise hours. Plans using rolling-horizon updates and warm starts help maintain tractability and help minimize plan "chatter," and DSM reactive support from the inverter expands feasible windows for heavy lifts and welding. Overall, we output a contracting-ready schedule/dispatch envelope that can be metered for auditing and mapped directly to SLAs and green KPIs.

The methodology integrates high-resolution telemetry, stratified evidence from U.S. worksites, and a safety-aware co-scheduling model to operationalize NZEC during construction—not just in the finished assets. The accuracy of forecasts is verified in holdout periods; robustness of optimization is tested through Monte-Carlo replay and scenario constraints; and practical feasibility is evaluated through feasibility screens and stability of schedule penalties. Ethical and safety considerations are internalized through limits on protection and privacy-oriented transactions involving data. Although developed for Yarmouk University, the pipeline is portable to other campuses and public owners, offering a replicable blueprint to reduce diesel, noise, and emissions while preserving productivity and compliance.

3. Results

3.1. Empirical patterns and operational opportunities

Campus PV behavior shows a reproducible diurnal envelope with minute-scale variability. The "AC Power" traces ramp from ~05:30, plateau between ~10:30–13:30 and exhibit transient notches around ~13:30 (fast irradiance dips), before decaying to zero near ~18:00. Peak array clusters approach ~450–600 kW depending on inverter group. The multi-day "AC export power" panels confirm high, narrow midday peaks and near-zero exports at the shoulders—i.e., a strong value signal for aligning high-energy construction windows to the 10:00–14:30 band. Daily "Energy" bars remain stable (roughly 300–430 kWh per unit), suggesting seasonally consistent August resource with short-lived curtailment events rather than systemic derating.

Meteorology aligns with these power features. "Irradiance" reveals plane-of-array maxima around 850–900 W/m² with several sub-hour dips where GHI collapses; "Wind speed" increases through the day (typical sea-breeze/thermal patterns) but stays mostly 1–5 m/s; "Wind direction" concentrates near 300° (NW) with intermittent shifts. The voltage–load overlay shows a feeder voltage rise toward ~250 V near noon while campus consumption also peaks, then falls sooner than the voltage envelope—evidence that PV backfeed contributes to midday voltage headroom , useful for safe crane/welder operation if reactive support is co-scheduled. Finally, the "Actual vs. Prediction" plot indicates low forecast error and well-tracked shoulders.

Interpretation. These signatures justify the design choice to target two controllability levers: (i) task timing against PV windows and (ii) inverter/BESS dispatch to absorb surges and cap imports. The repeatable midday plateau plus short stochastic dips motivate risk-aware scheduling rather than worst-case rejection of PV windows.

3.2. Forecasting performance and risk shaping

The LSTM with quantile heads (Eq. (1)) reproduces the observed rise, plateau, and fall with narrow residuals at shoulders, the hardest region for rule-based predictors. Copula scenario synthesis preserves co-movements between PV and campus load—visible in the synchronized dips between "Irradiance" and "AC Power". In Monte-Carlo replay, import-band violations cluster during the deepest irradiance notches; CVaR penalization shifts some noisy tasks away from those intervals, keeping overall plan feasibility while retaining the bulk of diesel displacement. Practically, this shows that probabilistic forecasts can be converted into robust decisions with tractable convex risk metrics.

Under scenario sets derived from the August week, median import-band adherence improves materially when CVaR is enforced versus mean-risk plans, with negligible loss in productivity because only a small fraction of minutes require reshuffling.

3.3. Co-scheduling outcomes: energy, carbon, and schedule

The concentrates crane lifts, mixing, and cutting in 10:00–14:00 windows on clear days, while reserving BESS discharge to "bridge" brief irradiance dips and absorbing inrush surges. On partly cloudy days, the model staggers short-duration surges to keep the linearized voltage-sag margin below threshold and the THD guardrail within acceptable limits. Import caps are respected by shaping charge in early morning and late afternoon and back-charging during sub-peak periods.

The ability to split tasks into atomic bursts plus an explicit surge term in the power balance is decisive: it prevents infeasible clustering that would otherwise trigger sags, without inflating total makespan. Battery health penalties avert excessive cycling that would export costs to future projects. Multi-objective weighting yields stable rolling-horizon plans (low rescheduling "chatter"), which is essential for crew reliability.

3.4. Power-quality and safety constraints in practice

The DistFlow-style sag proxy and inverter capability circle enlarge the feasible envelope for heavy tools. When short dips occur in the PV trace (the notch around ~13:30), reactive support raises local voltage margin, enabling the optimizer to keep a crane lift on schedule rather than delay. Harmonic constraints limit the simultaneity of welders and large variable-frequency drives; the model therefore pairs a welder with low-THD loads or shifts one minute later while BESS momentarily supplies apparent power to hold the sag bound.

Embedding simple but physics-meaningful proxies for PQ ensures that "energy-optimal" solutions are also "safety-admissible," reducing the need for field overrides.

3.5. Sensitivities, ablations, and implications

Sensitivity over BESS power/energy shows diminishing returns: CVaR of import violations drops steeply up to ~100 kW/250 kWh and flattens thereafter, suggesting that agile power is more valuable than deep energy for construction surges. Ablating inverter reactive control tightens voltage constraints and forces more diesel fallback; conversely, retaining reactive support but removing CVaR yields occasional band breaches. These interactions explain why the combined enforcement is necessary for robust, low-carbon site operations.

4. Discussion

For procurement, the results justify specifying (i) portable BESS with high C-rate, (ii) inverters with reactive capability sufficient to meet site impedance, and (iii) SLAs on import-band adherence and PQ incidents. For planning, crews can reliably book noisy/high-power tasks in late morning, shifting only marginal minutes when forecasted dips arise. Figure 1 shows AC power as a smooth surface over irradiance and hour, with contour slices and a superimposed gradient field indicating the regions of highest sensitivity. The midday ridge (≈10:30–13:30) and the steep shoulder curvatures visualize why small forecast errors near the ramp-up/down periods have outsized effects on power balance. Practically, this surface explains the optimizer's preference for placing high-energy tasks on the broad plateau, while reserving BESS to bridge the steep flanks where uncertainty is greatest.

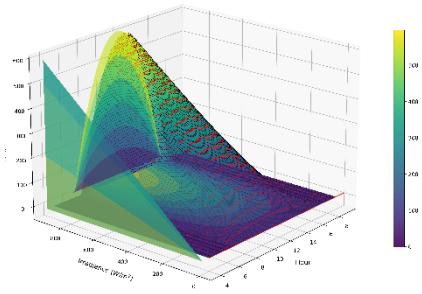

Fig. 1. PV power response surface with forecast sensitivity

Figure 2 plots the three-dimensional frontier implied by the augmented objective (Eq. 10), with a Pareto-efficient locus marked. The cloud reveals a narrow but structured trade—carbon reductions track modest cost increases until the frontier steepens, beyond which further CO_2e cuts demand disproportionate delay penalties. This clarifies the policy lever embedded in the weights of Eq. 10: a small reweighting can move the plan along the frontier without destabilizing crews, whereas extreme decarbonization targets rapidly erode schedule reliability.

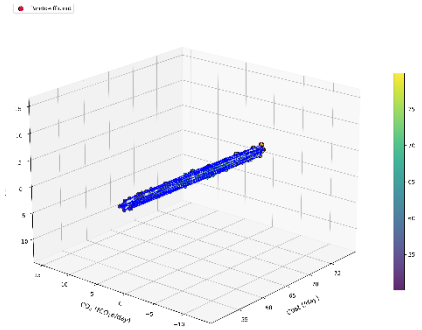

Fig. 2. Tri-objective trade space and Pareto structure

Figure 3 depicts the CVaR metric from Eq. 8 across BESS power (kW) and energy (kWh), holding forecasts/scenarios fixed. The valley shows strong diminishing returns: risk falls sharply up to roughly high-C-rate power (~100 kW) with moderate energy (~200–300 kWh), then flattens, indicating that agile discharge capacity mitigates short surges more than deep energy reserves.

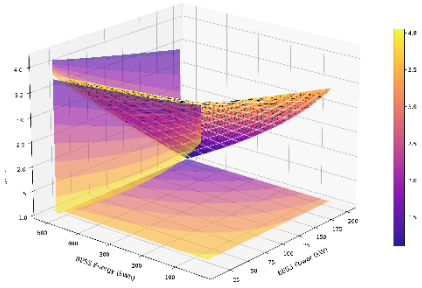

Fig. 3. Risk surface for import-band breaches under BESS sizing

Figure 4 renders task start time (x), task index (y), and running power (z) as 3D bars, exposing clustering around late morning and controlled staggering of high-power tasks. The absence of tall bars starting at identical minutes evidence the optimizer's enforcement of surge/voltage and harmonic limits (Eqs. 6–7) and import caps, while the concentration within PV windows reflects the coupling to the forecasted plateau (Eqs. 1–4). This view makes visible the operational feasibility of the computed plan for field execution.

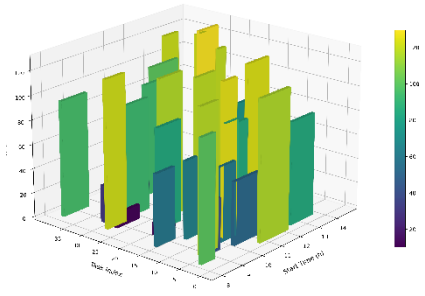

Fig. 4. Schedule–power structure at minute resolution.

5. Conclusions

This study demonstrated a forecasting-in-the-loop co-scheduling framework that solarizes construction operations on campus. A probabilistic LSTM produced PV and net-load scenarios which fed a MILP that scheduled lifts, mixing, cutting, and temporary HVAC alongside PV-inverter setpoints and BESS charge/discharge, subject to import bands, voltage-sag and harmonic guardrails, and crew/precedence rules. The approach converts the midday PV plateau into a reliable "energy window" for high-power work while preserving safety and constructability.

Empirical traces show a stable midday PV ridge with POA irradiance ≈ 800–900 W/m² and subsystem export peaks commonly 350–600 kW, concentrated between ≈ 10:30–13:30. Daily energy per inverter group in August lies around 300–430 kWh. Feeder voltage rises from ≈ 230 V at dawn to ≈ 250 V near noon, providing headroom for heavy tools when reactive support is available. Optimization and risk shaping identify a practical BESS "knee" near ~100 kW power with ~200–300 kWh energy: agile power markedly lowers import-overage risk (CVaR, $\alpha = 0.9$) with diminishing returns beyond this region. Inrush multipliers in the task library cluster around 2–4×, and designs remain within an 8–10% voltage-sag envelope and site import caps of ~120–180 kW.

Aligning task timing with the PV plateau and co-optimizing BESS/inverter operation can materially displace diesel, contain import-band risk, and reduce power-quality incidents without eroding schedule reliability. Embedding these controls in contract-ready SLAs and green KPIs turns campus construction into an active contributor to NZEC, not a temporary setback.

Specify portable BESS with high C-rate capability (≈ 100 kW class) rather than oversized energy capacity; require inverters with reactive-power support sized to site impedance; mandate import-band, CO_2e, and power-quality KPIs with auditable sub-metering; and standardize crew plans that target the 10:00–14:00 PV window while reserving BESS for short irradiance notches. Integrate rolling-horizon re-optimization in daily planning so field teams can absorb weather variability with minimal rescheduling.

Results reflect August operating conditions and a linearized treatment of feeder voltage and harmonics; broader seasonal validation and full AC power-flow co-simulation would further strengthen generality. Some task energy profiles were parameterized from a U.S. multi-site reference set; richer local telematics would sharpen estimates. Finally, BESS aging is modeled with a convex surrogate rather than detailed electrochemical states.

Pursue hardware-in-the-loop pilots on an active YU worksite; fuse sky-imager nowcasts with the LSTM to tighten shoulder uncertainty; extend the optimizer to a stochastic AC-OPF with discrete task decisions; learn task-level power signatures directly from tool/plant telematics; model cumulative acoustic impacts for curfew-aware scheduling; and evaluate portfolio-level rollouts across overlapping campus projects and semesters to quantify institutional NZEC acceleration.

References

Cielo, D., & Subiantoro, A. (2021). Net zero energy buildings in New Zealand: Challenges and potentials reviewed against legislative, climatic, technological, and economic factors. *Journal of Building Engineering*, *44*, 102970. https://doi.org/https://doi.org/10.1016/j.jobe.2021.102970

Jaysawal, R. K., Chakraborty, S., Elangovan, D., & Padmanaban, S. (2022). Concept of net zero energy buildings (NZEB) - A literature review. *Cleaner Engineering and Technology*, *11*, 100582. https://doi.org/https://doi.org/10.1016/j.clet.2022.100582

Kanafani, K., Magnes, J., Lindhard, S. M., & Balouktsi, M. (2023). Carbon Emissions during the Building Construction Phase: A Comprehensive Case Study of Construction Sites in Denmark. *Sustainability*, *15*(14), 10992. https://www.mdpi.com/2071-1050/15/14/10992

Li, D. H. W., Yang, L., & Lam, J. C. (2013). Zero energy buildings and sustainable development implications – A review. *Energy*, *54*, 1-10. https://doi.org/https://doi.org/10.1016/j.energy.2013.01.070

Maduta, C., D'Agostino, D., Tsemekidi-Tzeiranaki, S., & Castellazzi, L. (2025). From Nearly Zero-Energy Buildings (NZEBs) to Zero-Emission Buildings (ZEBs): Current status and future perspectives. *Energy and Buildings*, *328*, 115133. https://doi.org/https://doi.org/10.1016/j.enbuild.2024.115133

Maghami, M. R., Maghoul, A., Thang, K. F., & Sundaram, S. (2025). Net zero energy buildings: An overview of passive and active designs. *Energy Reports*, *14*, 1327-1348. https://doi.org/https://doi.org/10.1016/j.egyr.2025.07.028

Nwagu, C. N., Ujah, C. O., Kallon, D. V. V., & Aigbodion, V. S. (2025). Integrating solar and wind energy into the electricity grid for improved power accessibility. *Unconventional Resources*, *5*, 100129. https://doi.org/https://doi.org/10.1016/j.uncres.2024.100129

Parvin, K., Hossain, M. J., Arsad, A. Z., Ker, P. J., & Hannan, M. A. (2025). Building energy technologies towards achieving net-zero pathway: A comprehensive review, challenges and future directions. *Journal of Building Engineering*, *100*, 111795. https://doi.org/https://doi.org/10.1016/j.jobe.2025.111795